Representation of climate change in flood frequency estimation

Solomon S. Demissie and Conleth Cunnane
Department of Engineering Hydrology, National University of Ireland, Galway, Ireland

Abstract

This study presents a simplified method to account climate change impact in the conventional flood frequency estimation procedures. A stochastic cluster point process model known as the Modified Bartlett-Lewis Rectangular Pulses Model (MBLRPM) has reproduced the rainfall process satisfactorily. The evaporation series, which is less important in the context of flood in wet catchments with negligible snowfalls, is fitted to an Auto-Regressive Moving Average model, ARMA (1,1). The rainfall-runoff transformation of the catchments in this study is well captured by the revised Soil Moisture Accounting and Routing (SMARG) conceptual model. Monthly dimensionless precipitation scenario profiles are derived from ECHAM4/OPYC3 GCM output. Stochastic downscaling employed to represent precipitation scenarios in the MBLRPM. Then, a continuous simulation scheme was organized from components of the MBLRPM, the ARMA (1,1), the SMARG, the stochastic downscaling routine, and from flood frequency processor. Precipitation scenarios that cover the plausible ranges of the General Circulation Models (GCMs) estimate and some scaling concepts are hypothesized, and introduced in to the rainfall process by perturbing the MBLRPM parameters. In order to investigate the impact of climate change on the flood frequency, calibrated parameters of the MBLRPM, the ARMA (1,1) and the SMARG models, and the dimensionless precipitation scenario profiles are routed through the continuous simulation scheme. A climate change correction growth curve for flood frequency is then developed.

Résumé

Cette étude présente une méthode simplifiée pour intégrer les changements climatiques dans les procédures classiques d´estimation des fréquences de crue. Un modèle stochastique, connu sous le nom de *Modified Barlett-Lewis Rectangular Pulses Model* (MBLRPM) a reproduit de facon satisfaisante le phénomène des précipitations. Les chroniques d´évaporation, cette derniere étant moins importante pour les crues se produisant dans des bassins versants humides peu soumis aux chutes de neiges, ont été en adéquation avec un modèle nomme *Auto-regressive Moving Average model*, ARMA (1,1). La transformation des précipitations en ruissellement sur le bassin versant concerné par l´étude est bien rendue par le modèle conceptuel appelé *Soil Moisture Accounting and Routing* (SMARG). Chaque mois, les profils de scénarii de précipitation, sans dimensions, sont calculés a l`aide du modèle ECHAM4/OPY3 GCM, qui fournit un résultat global. Ce résultat a éte adapté pour le modèle MBLRPM, fonctionnant à une échelle géographique plus locale.. Puis, un programme de simulation continue a été mis en oeuvre à partir des composants du MBLRPM, du ARMA (1,1) du SMARG, du programme stochastique et du programme d´analyse de fréquences de crue. Nous avons supposé que les scénarios de précipitation couvrent l´étendue plausible des estimations du *General Circulation Models* (GCMs) et que les concepts d´échelle sont vérifiés, et les avons introduits dans le modèle de pluie en modifiant les paramètres du MBLRPM. Pour étudier l´impact des changements climatiques sur les fréquences de crue, les paramètres étalonnés des modèles du MBLRPM, du ARMA (1,1) et du SMARG, ainsi que les profils de scénarios des précipitations sans dimension sont introduits dans le programme de simulation continue. Une courbe corrigeant les fréquences de crue en fonction des changements climatiques peut alors être définie.

1. Introduction

Design flood estimation is a principal component in the study, design and management of water resource projects that are planned to achieve economical and safe water control and/or use. The most widely applied procedure for this purpose is an event-based flood frequency estimation in which future relationships between flood quantile and its frequency of occurrence is estimated from statistical analysis of observed historical events. The analysis might be done either at-site or at regional level (Cunnane, 1988; Hosking and Wallis, 1997). The second class of methodology for flood frequency estimation is a derived distribution approach, which is pioneered by Eagleson (1972). The probabilistic distribution of flood flows is determined from the density functions of climatic and hydrologic variables. This method suffers from the simplified assumptions made about the distribution and interaction of these variables for the purpose of mathematical tractability (Hebson and Wood, 1982; Diaz-Granados et al., 1984;

Bierkens and Puente, 1990). The most appealing but not fully investigated approach to flood frequency estimation is reported to be continuous simulation modeling (IH, 1999). The method simulates catchments water balance continuously by routing continuous climatic inputs through moisture accounting hydrological models. Different investigation carried out recently proved the promising potential of the method for land use and climate change impact assessment studies (Calver and Lamb, 1996; Blazkova and Beven, 1997; Lamb, 1999, Cameron et al., 1999; Demissie, 1999; Hashemi et al., 2000; Loukas et al. 2002; Yu et al. 2002).

All the above procedures estimate the magnitude of flood flow expected to occur at a specified return period from the current hydro-meteorological variables. But Global Circulation Models (GCMs) are forecasting pronounced variation in climatic variables under different integrations of greenhouse gas emission scenarios. For example, the main flood producing variable, precipitation, shows a general increasing trend in autumn and winter in the Northern Hemisphere mid- and high- latitudes (IPCC, 2001). Therefore, it is evident that flood frequency would be affected by changes in annual precipitation variability and by changes in rainfall characteristics (intensity and duration). This calls for plausible and physically based approach to incorporate climate-induced changes in the conventional flood frequency estimation procedures.

Assessment of the effect of climate change on the hydrologic systems has been broadly approached in three different ways. The first category directly simulates GCM outputs through watershed water balance models (Kamga, 2001; Loukas et al., 2002). But GCM results are too crude to apply at catchment level due to uncertainties involved in coarse spatial resolution and in simplified parameterization of cloud cover and rainfall process. The second approach identifies trends in climatic variables from long historical records and generates future time series based on the current trend, which is used as an input for hydrological models (Yu et al., 2002). The drawback behind this method is the expectation of similar trends in present and future climatic variables, which lacks an account of social, economical and environmental changes and interaction between elements of the climate. The third methodology applies a downscaling mechanism that can transfer high-resolution GCM simulated variables into watershed levels either by nesting regional climate models over GCM outputs, by establishing statistical relationships between large-scale circulation patterns and local climatic variables (Brandsma and Buishad, 1997; Wilby et al., 1998; Conway and Jones, 1998), or by representing the changing pattern of the GCMs outputs in to the respective variables' stochastic process at the watershed level (Burlando and Rosso, 1991). The current study applies stochastic downscaling to plausible precipitation scenarios, percentage change of monthly precipitation, and then develops the corresponding flood frequency scenarios using continuous simulation modeling.

2. The Study Area and Data Sets

This study was conducted on Fergus river catchment at Ballycorey in County Clare, Ireland. It has a drainage area of 512 km^2. The catchment is mostly flat with karstic nature in the upper lands. The dominant land use patterns are more farmlands with some proportions of scrubland, coniferous plantation, natural woodland and mixed woodland around the outlet. The Burren National Park is located at the center of the catchment, which will preserve the land in its present state for long time. Small caves, scattered ponds, and minor lakes are the major hydro-geological features of the catchment. The stream networks and the lakes are concentrated at the lower half part of the catchment while the upper part is a karstic land.

The areal mean daily rainfall of the catchment is computed from the daily rainfall data of four meteorological stations: Carron, Corofin, Crushen and Kilmaley. The mean annual rainfall of the catchment is 1425 mm. Monthly potential evapo-transpiration from the nearby Shannon Airport synoptic station and mean daily flow from Ballycorey hydrological station (the outlet) from 1975 to 1999 inclusive are also used for calibration and verification of the rainfall-runoff model. The mean annual daily flow for this period was 10.25 m^3/s.

Monthly mean total precipitation prediction [1950 – 2099] from the German Max-Planck Institute's GCM (HCHAM4/OPYC3) for constant CO2 (control) and for greenhouse gas integrations of IS92a emission scenario is downloaded from the DKRZ ftp database organized on behalf of the IPCC Data Distribution Centre. From the data at a grid point close to the catchment (8.4375W, 51.4162N), dimensionless monthly profile of the changing factors of precipitation is established as discussed in section 4.2.

3. Modeling of Meteorological and Hydrological Variables

Continuous simulation study requires generation of input variables to the water-balance model and proper specification of the model. The common input variables are rainfall and potential evapo-transpiration. Therefore, it is necessary to model the rainfall process, the potential evapo-transpiration series and the rainfall-runoff transformation independently using the respective historical time series.

3.1. Stochastic rainfall modeling

The best representation of rainfall process can be achieved through cluster point process models. The parameters of these models physically explain the rainfall process. Previous studies done by Khaliq (1995) and Khaliq and Cunnane (1996) showed that Modified Bartlett-Lewis Rectangular Pulses model (MBLRPM) performs well in Ireland. Following Rodriguez-Iturbe et al. (1988), the MBLRPM defined as follows. Storm origins arrive in a Poisson process of rate λ. Each storm origin is followed by a Poisson process of rate β of cell origins. The process of cell origins terminates after a time that is exponentially distributed with parameter γ. The durations of the cells are exponentially distributed random variables with parameter η and each cell depth is a random constant exponentially distributed with mean μ_X. The η values for distinct storms are independent random variables having a common gamma distribution with index α and scale parameter ν. In order to change the mean inter-arrival interval of cells and the mean storm duration time randomly with cell duration, dimensionless parameters $\kappa = \beta/\eta$ and $\phi = \gamma/\eta$ are introduced. The number C of cells per storm has a geometric distribution with mean $\mu_C = 1 + \kappa/\phi$. Generally, the MBLRPM has six parameters: λ, κ, ϕ, ν, α and μ_X. The full analytical expression of the first- and second-order properties for both depth and aggregated process are given in Rodriguez-Iturbe et al. (1987 and 1988).

The MBLRPM is applied to the areal mean daily rainfall of the catchment on monthly basis so that the stationary assumption of the model could be satisfied. The monthly empirical estimates [1975 – 1999] of mean, variance, lag-1 autocorrelation and dry proportion at 1-day and 2-days levels of aggregation are matched with the respective analytical expressions of the aggregated process for parameter estimation. Rosenbrock's method of non-linear unconstrained optimization algorithm is used to minimize a weighted least square objective function. The estimated and validated parameters are listed in Table 1 and the performance of the model is displayed in Figure 1.

Table 1. Estimated parameter values of the MBLRPM for daily rainfall of Fergus Catchment.

Month	λ (day^{-1})	κ	ϕ	ν (day)	α	μ_X (mm.day^{-1})
Jan	0.50636	0.13078	0.02489	1.86020	30.42782	25.36800
Feb	0.52266	0.14836	0.02323	1.13195	31.30844	27.01556
Mar	0.64982	0.08860	0.02279	1.64738	42.55167	31.89741
Apr	0.12901	0.12380	0.01599	5.25120	24.88441	10.94763
May	0.37741	0.15949	0.03353	1.51322	30.87696	22.05181
Jun	0.52997	0.05628	0.03030	1.01563	33.03481	56.42801
Jul	0.43008	0.06357	0.01907	1.24320	36.35539	41.04176
Aug	0.24244	0.06316	0.01080	1.76717	28.24481	37.46912
Sep	0.41144	0.04433	0.01253	1.21746	35.65247	59.20959
Oct	0.49870	0.04786	0.00838	0.79702	44.67371	79.01536
Nov	0.55715	0.05392	0.01359	0.95851	35.65328	59.14481
Dec	0.10594	0.17143	0.00784	3.37363	22.42182	13.52191

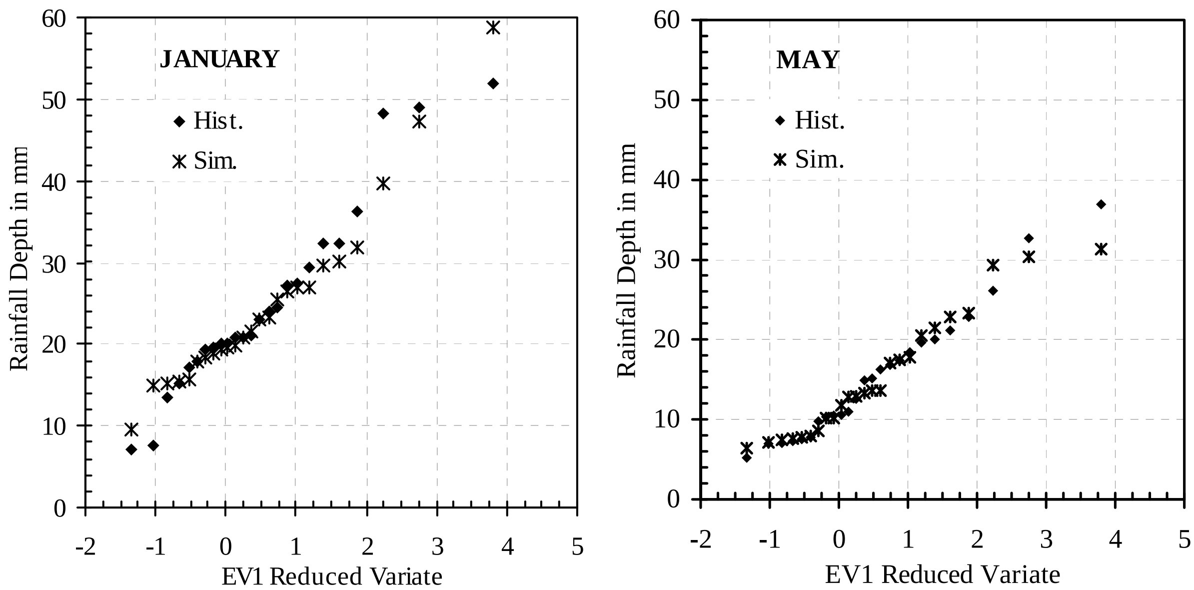

Figure 1. Comparison of historical and MBLRPM simulated annual maximum areal mean rainfall for heaviest (January) and the lightest (May) months.

3.2. Evapo-transpiration series modeling

The autocorrelation and partial autocorrelation functions of the series suggest that first-order Auto-Regressive and first-order Moving Average process, ARMA (1,1), suffices to model this time series. If the evaporation series E_t has a mean of μ, the ARMA (1,1) model can be expressed as:

$$(1-\phi B)(E_t-\mu)=(1-\theta B)\sigma_a^2\xi_t, \qquad (1)$$

where, ϕ is the auto-regressive parameter, θ is moving average parameter, B is the backward shift operator, σ_a^2 is the variance the white noise process, and ξ_t is the standard normal ordinate. For the purpose of satisfying the stationary condition, the modeling exercise is performed on monthly basis. Table 2 portrays the estimated and validated model parameters.

Table 2. Estimated parameter values of ARMA (1,1) model for daily evapo-transpiration.

Month	ϕ	θ	σ_a^2	μ
Jan	0.97163	0.03539	0.11246	0.280
Feb	0.96082	-0.30986	0.14216	0.708
Mar	0.96533	0.08535	0.09385	1.169
Apr	0.96567	-0.18083	0.11852	2.014
May	0.95325	0.14513	0.23423	2.765
Jun	0.97945	-0.25724	0.25959	3.065
Jul	0.97720	0.06263	0.30748	2.803

Table 2 continued …

Month	ϕ	θ	σ_a^2	μ
Aug	0.96528	0.08481	0.22504	2.364
Sep	0.96901	-0.33162	0.13909	1.690
Oct	0.96899	0.03861	0.06239	0.804
Nov	0.96310	-0.21100	0.06703	0.320
Dec	0.96594	0.16786	0.07963	0.140

3.3. Rainfall-runoff modeling

Since the proposed continuous simulation modeling involves generation of lengthy time series as many realization as possible, the rainfall-runoff model should not be complicated and computationally costly. Therefore, a lumped conceptual model developed in this Department and whose performance in such climatic regions was found to be reliable is selected for this study. Its development starts from the original Layers Model of O'Connell et al. (1970), which is modified to SMAR (Soil Moisture Accounting an Routing) model by Khan (1986). Then, Liang (1992) introduced the concept of separating quick and slow runoffs in the SMAR model and came up with the SMARG model. Tan and O'Connor (1996) and Mingkai (1996) made further improvement on this model. But, the SMARG version that is available in the UCGMODEL package is adopted in the current study.

The SMARG model, as most conceptual models, has two major components; water balance and routing components. The water balance component simulates non-linear processes involved in runoff generation on conceptual basis and hence generates surface and ground water runoffs from rainfall and evaporation input. Six parameters are involved in the process: (1) T converts evaporation input series to model-estimated potential evaporation series, (2) H determines the proportion of the generated direct runoff from excess rainfall, (3) Y is the maximum infiltration capacity depth, (4) Z is the soil moisture storage depth of the layers, (5) C is the evaporation decay coefficient of the soil moisture storage layers in such a way that less evaporation occurs from deeper layer, and (6) G determines the proportion of the ground water generated runoff from moisture in excess of soil storage capacity. The routing component transforms the generated surface and ground water runoffs into discharge at the catchment outlet through linear time-invariant storage systems of Nash cascade of N equal reservoirs and simple linear reservoir respectively. This attenuation and diffusion process adds three more parameters: (1) N is a shape parameter and (2) NK is a scale parameter of a gamma unit impulse response of the Nash cascade reservoirs, and (3) Kg is the storage coefficient of the ground water simple linear storage. All together, the SMARG model has nine parameters.

Using the twenty-five years [1975 – 1999] of synchronous daily data of rainfall, evapo-transpiration and stream flow of the catchment; the SMARG model was calibrated and verified for all sets of parameters so that all features of the model can be used in the simulation study. After some preliminary modeling exercises, a memory length of 15 days, a warm up period of 60 days, a calibration period of 17 years and a verification period of 8 years and the Rosenbrock's optimization algorithm are used for parameter estimation. The Nash-Sutcliffe's efficiency criterion (R^2 in %) of 92.70 and 91.31 achieved during calibration and verification respectively. Table 3 shows the list and estimated values of the parameters. The graphical display of the observed and simulated flow series shown in Figure 2 confirms the good performance of the model for the Fergus catchment.

Table 3. Optimized parameters of the SMARG model for Fergus catchment.

Water Balance Component		Routing Component	
Parameter	Estimate	Parameter	Estimate
T	0.992929	N	2.18895
H	0.512684	NK	16.0486
Y	250.540	Kg	34.3327
Z	483.373		
C	0.564493		
G	0.699249		

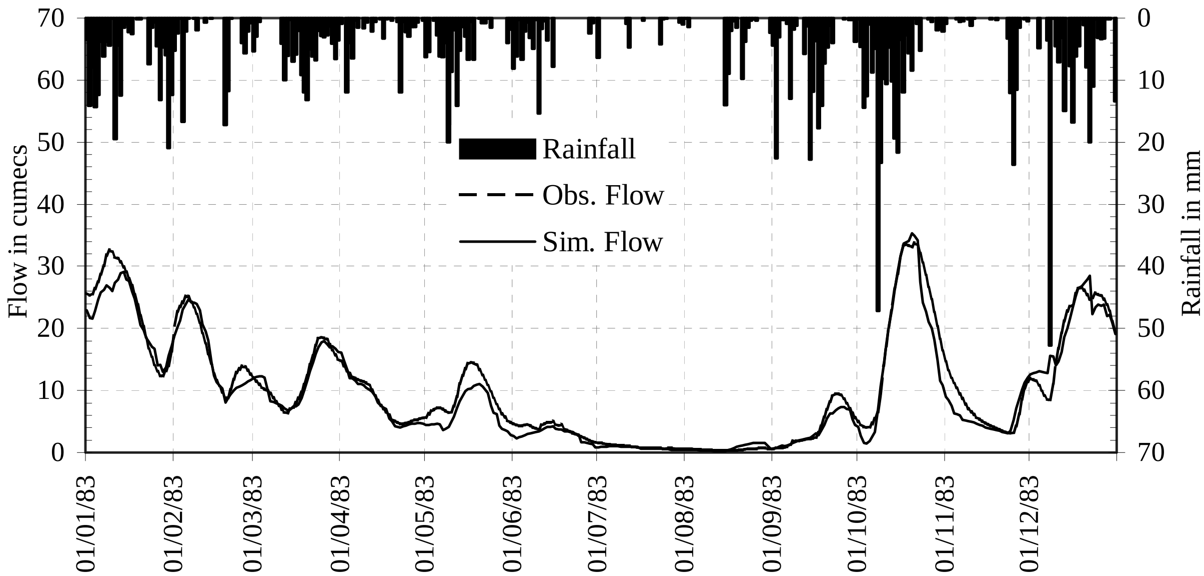

Figure 2. Comparison of observed and SMARG model simulated flow series for Fergus catchment.

4. Development of Climate Scenarios

The main objective of the present study is to develop flood frequency scenarios that can represent the effect of climate change on flow extremes from plausible ranges of climate scenarios known from GCM experiments using stochastic downscaling and continuous simulation modeling. However, floods from catchments that are wet all over the year with negligible snowfalls are less sensitive to changes in evapo-transpiration. This was verified by simulation studies conducted on the Fergus catchment. It is well understood that precipitation is the main deriving element of the water balance and plays the major role in flood producing mechanisms. Therefore, the impact of climate change on flood flows could be investigated by downscaling precipitation scenarios into the rainfall stochastic process and then to watershed process.

4.1. Stochastic downscaling of precipitation scenarios

Following the pioneer work of Burlando and Rosso (1990), precipitation scenarios in terms of percentage change or rate of change of mean monthly precipitation between climate-enhanced and control GCM simulations, stochastic modeling and scaling concepts could be applied to predict future precipitation patterns at operational resolution level. Burlando and Rosso (1991) introduced the methodology using Neyman-Scott Rectangular Pulses model to investigate the pattern of extreme storm rainfall under climate change. In this study the theoretical approach is further developed for the Modified Bartlett-Lewis Rectangular Pulses model. The scaling relationship between the second-order properties of the aggregated rainfall depth process is used to find the rate of change of the variance from the mean, the adopted scenario. The scaling exponents of central moments (mean and variance) of the 12 months were not significantly different from each other. The non-seasonality nature of the scaling exponent is taken as sufficient condition to assume the same value during the current and future climate. From empirical analysis of the areal mean daily rainfall of the catchment at different levels of aggregation (h), the following scaling relationship was obtained (see Figure 3a):

$$\mathrm{var}[Y_i^h] = c\left\{E[Y_i^h]\right\}^{2\psi}, \text{ where c = 5.42599 and } \psi = 0.68815. \tag{2}$$

Consequently, changing factor of variance $R_{\sigma}{}^2$ can be written as in terms of the precipitation scenario, changing factor of mean R_m, as follow:

$$R_{\sigma^2} = (R_m)^{2\psi} \tag{3}$$

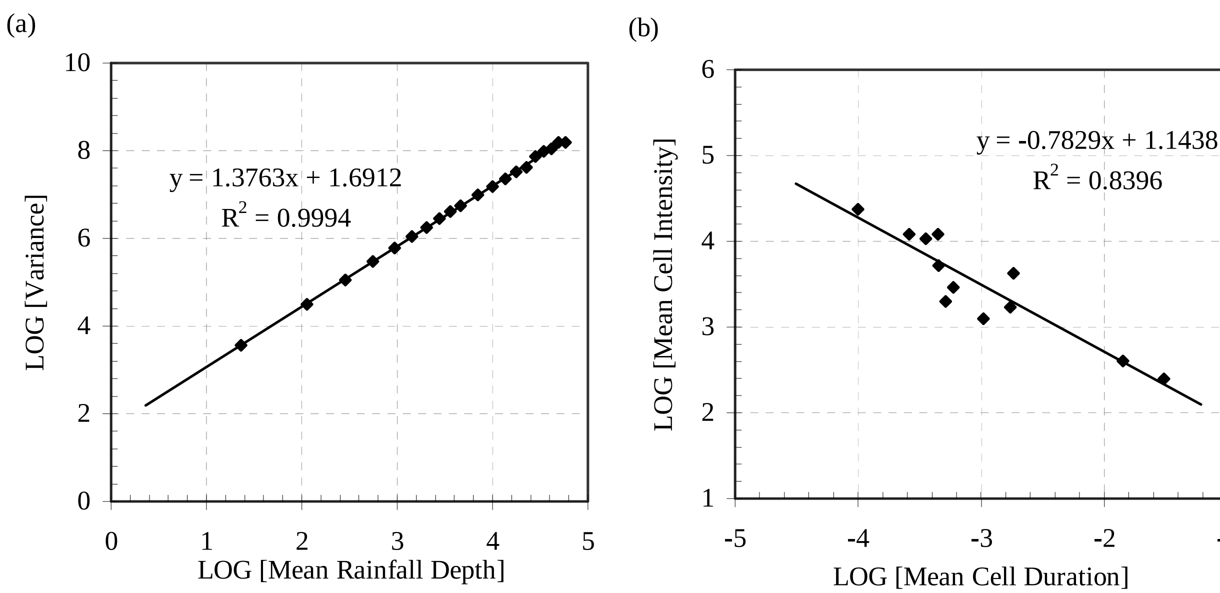

Figure 3. Scaling relationship of (a) central moments and (b) rain cell characteristics for daily areal rainfall of Fergus catchment.

Rainfall depth is a highly fluctuating process. Most hydrological applications like DDF use the aggregated (integrated) values of this fluctuating process. The scale of fluctuation gives the level of aggregation required to obtain stable (low variance) estimates of the mean of the fluctuating rainfall depth process (Vanmarcke, 1983). For the MBLRPM, the scale of fluctuation θ can be given by:

$$\theta = \frac{2\nu(\mu_C + 1)}{(\alpha - 2)\left[2 + \frac{\kappa}{\phi + 1}\right]} \tag{4}$$

If we assume a linear transformation between the current, $(.)_o$ and the climate-induced, $(.)_e$ rainfall depth process, the following relationship would be satisfied as shown by Vanmarcke (1983).

$$\frac{\sigma_0^2\theta_0}{m_0^2} = \frac{\sigma_e^2\theta_e}{m_e^2} \tag{5}$$

Combining equations 2 and 4, the changing factor of the scale of fluctuation can be expressed as:

$$R_\theta = (R_m)^{2(1-\psi)} \tag{6}$$

When Redriguez-Iturbe et al. (1988) introduced the concept of randomness in cell duration parameter (η), the mean number of cells per storm, $\mu_C = 1+\kappa/\phi$, is kept constant without losing generality. Similarly, we can assume that μ_C will be the same in both the control and climate-induced systems. Then, it is easy to show that the changing factors of κ and ϕ are equal.

$$R_\kappa = R_\phi \tag{7}$$

The purpose of two of the six parameters of the MBLRPM (α and ν) is to randomly vary the gamma distributed cell duration parameter (η) from storm to storm. So, if we assume that the shape parameter α remains unchanged during climate enhancement, the cell duration will still vary due to the change in scale parameter ν. Moreover, the mathematical expression will be simplified to extractable level. Therefore,

$$R_\alpha = 1.0 \tag{8}$$

Different empirical studies and physical interpretation of the rainfall process confirms that average storm intensity is inversely related to its duration of occurrence. Koutsoyiannis and Foufoula-Georgiou (1993) suggested power relationship so that both the inverse relation and the scaling property could be exploited. Consequently, we are hereby assuming the same scaling relationship could occur between mean rain cell intensity, μ_x and mean rain cell duration, $E[\eta^{-1}] = \nu/(\alpha-1)$ in the MBLRPM structure. Figure 3b empirically verifies this assumption and yields a power relationship of:

$$\mu_X = d\left(\frac{\nu}{\alpha - 1}\right)^\delta \text{, where d = 3.1387 and } \delta = -0.7829. \tag{9}$$

From equations (8) and (9), the changing factor relationship between μ_X and ν can be written as:

$$R_{\mu_X} = \left(R_\nu\right)^\delta \tag{10}$$

Now we had changing factors for three second-order properties, mean, variance and scale of fluctuation, and for three theoretically sound assumptions that gave equations (7), (8) and (10). Then, after algebraic manipulation and application of simple optimization technique, the changing factors by which the six model parameters should be perturbed to represent the precipitation scenario into the stochastic rainfall process could easily be obtained.

4.2. Seasonal profile of precipitation scenarios

As the main purpose of this study is to figure out the amount by which flood magnitudes at different frequencies of occurrence will change when the rainfall changed by certain factor, it becomes necessary to set a reference season and monthly profile of precipitation changes. Almost all annual maximum floods in this country were observed in winter season (DJF). Therefore, percentage change of winter precipitation during climate change is hereafter taken as precipitation scenario. Since rainfall modeling is taking place in monthly basis, we have to devise a means to distribute this precipitation scenario to each month.

The monthly and seasonal percentage changes of precipitation from ECHAM4/OPYC3 GCM predictions of greenhouse gas and control integrations for different climatic times are computed for the nearby grid point as shown in Figure 4. Then, a dimensionless monthly precipitation scenario profile, whose ordinate values are listed in Table 4, is obtained from rescaling the mean monthly changing factors of precipitation by the mean winter changing factor. And this dimensionless profile is used to distribute the above defined precipitation scenario to the respective months in the continuous simulation experiment. Based on the precipitation changes observed from the GCM experiment shown in Figure 4, precipitation scenarios that include all possible future ranges are identified as –20%R, -15%R, -10%R, 0%R, +10%R, +15%R, +20%R and +25%R, and applied in the foregoing experiment. Hereinafter the 0%R precipitation scenario is known as reference precipitation scenario.

Table 4. Dimensionless monthly precipitation scenario profile derived from ECHAM4/OPYC3 GCM data.

Month	Profile Ordinate	Month	Profile Ordinate
Jan	1.01232	Jul	0.76435
Feb	1.00469	Aug	0.75891
Mar	1.04580	Sep	0.89647
Apr	0.79504	Oct	0.95380
May	0.85542	Nov	1.02349
June	0.83505	Dec	0.98428

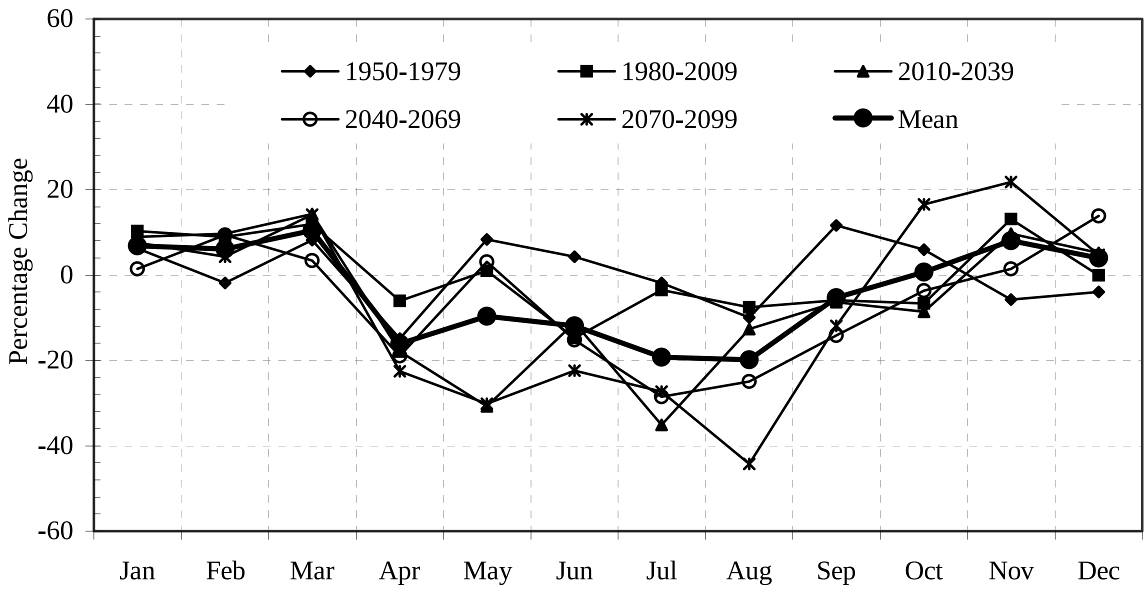

Figure 4. Monthly percentage changes of precipitation from greenhouse gas integration to control integration of the ECHAM4/OPYC3 GCM experiment at (8.4375W, 51.4162N) grid point.

5. Organization and Application of Continuous Simulation Scheme

The time series generator part of the MBLRPM and ARMA (1,1), the simulator component of the SMARG model, the precipitation downscaling routine, and flood frequency processor are combined together to form a continuous simulation scheme. The inputs to the scheme are the calibrated parameters of the three models, the dimensionless monthly precipitation scenario profile and the precipitation scenario as percentage change of winter rainfall. The number of simulations (realizations), the length of the time series and the starting year of simulation are off course part of the input. The scheme was tested and verified by its ability to reproduce the observed annual maximum annual flow series from 1000 simulations of 25 years each for the current climate. The result displayed in Figure 5 confirms the dependability of the scheme for the proposed climate change impact assessment study.

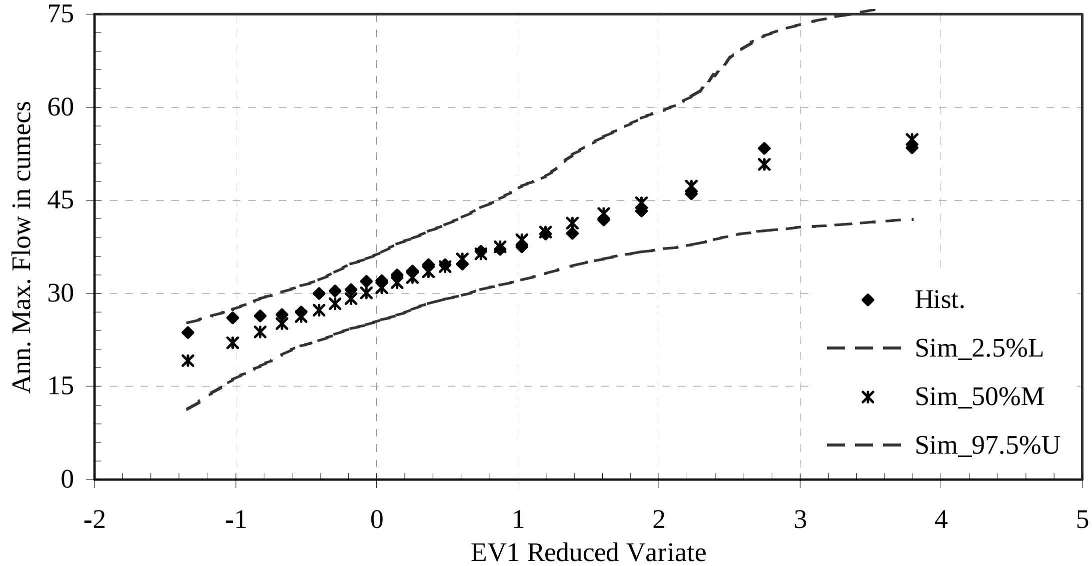

Figure 5. Comparison of the historical and the continuous simulation scheme results of annual maximum flow series. Dashed lines show the 95% confidence intervals of the simulation results.

For each of the above-hypothesized precipitation scenarios, 1000 simulations of 100 years continuous flow series are generated and the corresponding annual maximum flow (AMF) series are selected and analyzed non-parametrically. The percentage changes of the annual maximum flow series of a given precipitation scenario form the respective series of the reference precipitation scenario are computed for all of the above scenarios. These percentage changes can be interpreted as AMF scenarios at the specified frequency of occurrence. Further normalizing the AMF scenarios by the respective precipitation scenarios gives dimensionless factors that quantify the impact of climate change on flood flows in terms of precipitation changes. These factors for different frequency of occurrences produced growth curves, as shown in Figure 6, which can be applied as a climate change correction to flood frequencies estimated from the current climatic data by any conventional method.

6. Discussion of Results and Conclusions

The continuous simulation scheme assembled for this study requires higher level of computing power and takes appreciable time to get the result. Therefore, it is not feasible to adopt such simulation schemes for practical design flood estimation works. Since precipitation scenarios for a certain region can be estimated from GCMs output, the developed climate change correction growth curves can be used with conventional flood frequency analysis methods for design flood estimation. Hence engineers and technicians engaged in the design and operation of storm sewers, culverts, rain water harvesting reservoirs, weirs and other water resources projects can apply climate change corrections to design floods estimated from monographs, charts and conventional methods using such curves developed for their region. For example, if the precipitation scenario is 20%R and the return period considered is 20 years (EV1 reduced variate of 1.97), one can read 0.95 from Figure 6 and get 19% (=0.95×20%) as the amount by which the 20-year flood should be increased.

The simulation result summarized in Figure 6 shows that there is no linear relationship between precipitation and annual maximum flood scenarios. It also reveals that low return period floods are more sensitive to climate change than high return period floods. This might be due to the degree of wetness of the cathment at different flood frequencies. If the catchment is wetter, its dynamics in less affected by changes in precipitation and produces higher floods. So, the derived curves exhibit a physically possible pattern.

Although some assumptions and monthly mean changes in GCM precipitation outputs are employed in the downscaling process, this preliminary result of our on going study gives an indicative framework for incorporating climate change in flood frequency estimation procedures. We hope that most of the limitations of this work will be clarified at the final stage of the study.

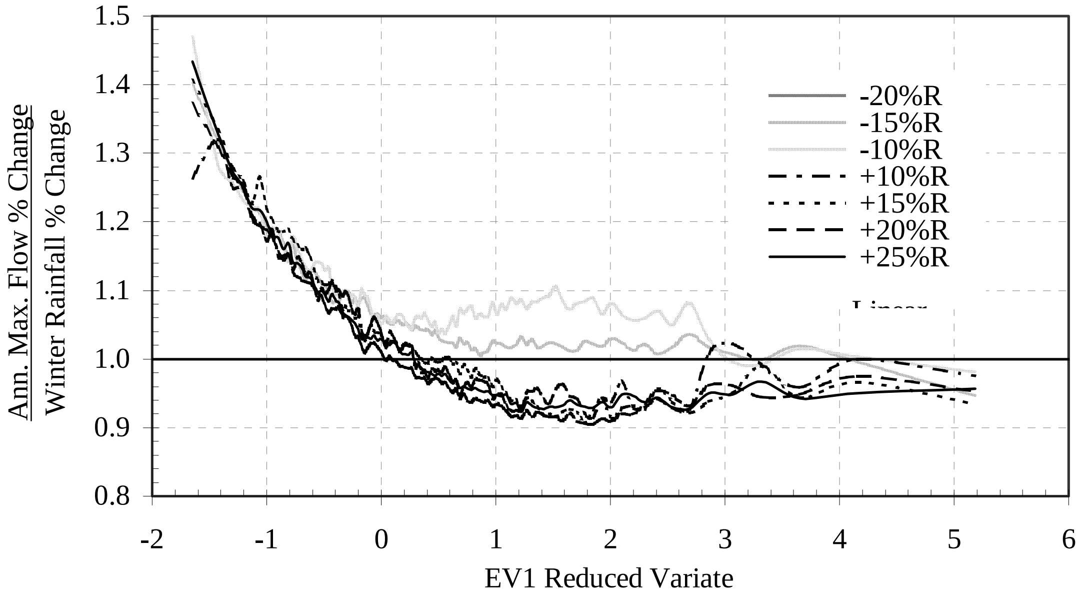

Figure 6. Climate change correction growth curves for flood frequency estimation.

Acknowledgments

This research has been supported by funding from Environmental Change Institute of the National University of Ireland, Galway as part of the Higher Education Authority Programme for Research in Third Level Institutions (HEA PRTLI) Cycle 2.

References

Bierkens, M.F. and Puente, C.E., 1990. Analytically derived runoff models based on rainfall point processes. Water Resour. Res., 26(11): 2653-2659.

Blazkova, S. and Beven, K., 1997. Flood frequency prediction for data limited catchments in the Czech Republic using a stochastic rainfall model and TOPMODEL. J. Hydrol., 195: 256-278.

Brandsma, T. and Buishand, T.A., 1997. Statistical linkage of daily precipitation in Switzerland to atmospheric circulation and temperature. J. Hydrol., 198: 98-123.

Burlando, P. and Rosso, R., 1991. Extreme storm rainfall and climate change. Atm. Res., 27: 169-189.

Calver, A. and Lamb, R., 1996. Flood frequency estimation using continuous rainfall-runoff modeling. Phys. Chem. Earth, 20(5-6): 479-483.

Cameron, D.J., Beven, K.J., Tawn, J. Blazkova, S. and Naden, P., 1999. Flood frequency estimation by continuous simulation for a gauged upland catchment (with uncertainity). J. Hydrol., 219: 169-187.

Conway, D. and Jones, P.D., 1998. The use of weather types and airflow indices for GCM downscaling. J. Hydrol., 212-213: 348-361.

Cunnane, C., 1988. Methods and merits of regional flood frequency analysis. J. Hydrol., 100: 269-290.

Demissie, S.S., 1999. Assessment of land use and climate changes on flood flows. M.Sc. Thesis, Department of Engineering, National University of Ireland, Galway.

Diaz-Granodos, M.A., Valdes, J.B. and Bras, R.L., 1984. A physically based flood frequency distribution. Water Resour. Res., 20(7): 995-1002.

Eagleson, P.S., 1972. Dynamics of flood frequency. Water Resour. Res., 8(4): 878-898.

Hashemi, A.M., Franchini, M. and O'Connell, P.E., 2000. Climatic and basin factors affecting the flood frequency curve: PART I – A simple sensitivity analysis based on the continuous simulation approach. Hydrol. Earth System Sci., 4(3): 463-498.

Hebson, C. and Wood, E.F., 1982. A derived flood frequency distribution using Horton order ratios. Water Resour. Res., 18(5): 1509-1518.

Hosking, J.R.M. and Wallis, J.R., 1997. Regional flood frequency analysis: an approach based on L-moments. Cambridge University Press.

Institute of Hydrology, 1999. Flood estimation handbook. Wallingford, UK.

IPCC, 2001. Climate Change 2001: impacts, adaptation and vulnerability. Downloaded from www.ipcc.ch.

Kamga, F.M., 2001. Impact of greenhouse induced climate change on runoff of the upper Benue river (Cameroon). J. Hydrol. 252: 145-156.

Khaliq, M.N. and Cunnane, C., 1996. Modeling point rainfall occurrences with the Modified Bartlett-Lewis Rectangular Pulses model. J. Hydrol., 180: 109-138.

Khaliq, M.N., 1995. Stochastic modeling of rainfall occurrences and its use for modeling effects of climatic changes on rainfall extreme values. Ph.D. Thesis, Department of Engineering hydrology, U.C.G., National University of Ireland.

Koutsoyiannis, D. and Foufoula-Georgiou, E., 1993. A scaling model of a storm hyetograph. Water Resour. Res., 29(7): 2345-2361.

Koutsoyiannis, D. and Foulfoula-Georgiou, E., 1993. A scaling model of a storm hyetograph. Water Resour. Res., 29(7): 2345-2361.

Lamb, R., 1999. Calibration of a conceptual rainfall-runoff model for flood frequency estimation by continuous simulation. Water Resour. Res., 35(10): 3103-3114.

Liang, G.C., 1992. A note on the revised SMAR model. Workshop memorandum, Department of Engineering Hydrology, U.C.G., National University of Ireland (unpublished).

Loukas, A., Vasiliades, L. and Dalezios, N., 2002. Potetial climate change impacts on flood producing mechanisms in Southern British Columbia, Canada using the CGCMA1 simulation results. J. Hydrol., 259: 163-188.

Mingkai, Q., 1996. Further development of the SMAR model – An improvement to the description of the overland flow process. M.Sc. Thesis, Department of Engineering Hydrology, U.C.G., National University of Ireland.

O'Connell, P.E., Nash, J.E. and Farrell, J.P., 1970. River flow forecasting through conceptual models, Part 2, The Brosna catchment at Ferbane. J. Hydrol., 10(4): 317-329.

Rodriguez-Iturbe, I., Cox, D.R. and Isham, V., 1987. Some models for rainfall based on stochastic point processes. Proc. R. Soc. London, A, 410: 269-288.

Rodriguez-Iturbe, I., Cox, D.R. and Isham, V., 1988. A point process model for rainfall: further developments. Proc. R. Soc. London, A, 417: 283-298.

Tan, B.Q. and O'Connor, K.M., 1996. Application of an empirical infiltration equation in the SMAR conceptual model. J. Hydrol., 185: 275-295.

Vanmarcke, E., 1983. Random fields: Analysis and Synthesis. MIT Press, Cambridge, Massachusetts.

Wilby, R.L., Hassan, H. and Hanaki, K., 1998. Statistical downscaling of hydro-meteorological variables using general circulation model output. J. Hydrol., 205:1-19.

Yu, P., Yang, T. and Wu, C., 2002. Impact of climate change on water resources in Southern Taiwan. J. Hydrol., 260: 161-175.